International Journal of Nanomedicine

Dovepress
open access to scientific and medical research

Open Access Full Text Article

ORIGINAL RESEARCH

Magnetic Removal of *Candida albicans* Using Salivary Peptide-Functionalized SPIONs

Bernhard Friedrich[1], Rainer Tietze[1], Michaela Dümig[2], Alexandru Sover[3], Marius-Andrei Boca[3], Eveline Schreiber[1], Julia Band[1], Christina Janko[1], Sven Krappmann[2], Christoph Alexiou[1,*], Stefan Lyer[1,4,*]

[1]Department of Otorhinolaryngology, Head and Neck Surgery, Section of Experimental Oncology and Nanomedicine (SEON), Else Kröner-Fresenius-Stiftung Professorship, Universitätsklinikum Erlangen, Erlangen, Germany; [2]Mikrobiologisches Institut – Klinische Mikrobiologie, Immunologie und Hygiene, Universitätsklinikum Erlangen, Friedrich-Alexander-Universität (FAU) Erlangen-Nürnberg, Erlangen, Germany; [3]Faculty of Engineering, Ansbach University of Applied Sciences, Ansbach, Germany; [4]Department of Otorhinolaryngology, Head and Neck Surgery, Section of Experimental Oncology and Nanomedicine (SEON), Professorship for AI-Controlled Nanomaterials, Universitätsklinikum Erlangen, Erlangen, Germany

*These authors contributed equally to this work

Correspondence: Stefan Lyer, Section of Experimental Oncology & Nanomedicine (SEON), Glückstraße 10a, Erlangen, 91054, Germany, Tel +49-9131-85-33142, Fax +49-9131-85-34828, Email stefan.lyer@uk-erlangen.de

Purpose: Magnetic separation of microbes can be an effective tool for pathogen identification and diagnostic applications to reduce the time needed for sample preparation. After peptide functionalization of superparamagnetic iron oxide nanoparticles (SPIONs) with an appropriate interface, they can be used for the separation of sepsis-associated yeasts like *Candida albicans*. Due to their magnetic properties, the magnetic extraction of the particles in the presence of an external magnetic field ensures the accumulation of the targeted yeast.

Materials and Methods: In this study, we used SPIONs coated with 3-aminopropyltriethoxysilane (APTES) and functionalized with a peptide originating from GP340 (SPION-APTES-Pep). For the first time, we investigate whether this system is suitable for the separation and enrichment of *Candida albicans*, we investigated its physicochemical properties and by thermogravimetric analysis we determined the amount of peptide on the SPIONs. Further, the toxicological profile was evaluated by recording cell cycle and DNA degradation. The separation efficiency was investigated using *Candida albicans* in different experimental settings, and regrowth experiments were carried out to show the use of SPION-APTES-Pep as a sample preparation method for the identification of fungal infections.

Conclusion: SPION-APTES-Pep can magnetically remove more than 80% of the microorganism and with a high selective host-pathogen distinction *Candida albicans* from water-based media and about 55% in blood after 8 minutes processing without compromising effects on the cell cycle of human blood cells. Moreover, the separated fungal cells could be regrown without any restrictions.

Keywords: *Candida albicans*, SPIONs, fungal sepsis, GP340, microbiological identification

Introduction

Fungal infections are a frequently underestimated clinical picture associated with both severe local and systemic inflammatory reactions. These microorganisms are known to cause a variety of host reactions that can lead to hypersensitivity disorders, toxic reactions and sepsis. Such types of infectious diseases, called mycoses, are categorized according to their causative agent (eg candidiasis, cryptococcosis, and aspergillosis) and primarily affect immunocompromised individuals. Furthermore, mycoses can also occur endemically, ie permanently localised geographically, like eg histoplasmosis, blastomycosis, coccidioidomycosis or penicilliosis.[1] Additionally, various factors such as viral pan- and endemics (HIV, SARS-CoV-2), an ageing society, increasing numbers of surgical procedures have increased the number of immunocompromised patients, who are prone to opportunistic infections.[2] As in the case

Received: 21 February 2023
Accepted: 7 May 2023
Published: 14 June 2023

of bacterial sepsis, there is also in mycoses an urgent need for faster and more sensitive diagnostics in order to start appropriate antimycosis treatment as soon as possible and to significantly increase the patient's chances of recovery. Especially in the case of candidiasis, the rather long-time spans until positive detection vary greatly. Clinically, the most rapid detection is usually that of *Candida tropicalis* with an average of 19 h, whereas the longest time for positive detection of a *Candida* species is that of *Candida glabrata* with an average of 75 h.[3] The most dominant and clinically most relevant yeast species to cause bloodstream infections is *Candida albicans* by far.[1,4–6] Here the medium time to detection is around 10 min. These examples demonstrate how important finding possibilities to accelerate fungal blood infections are.

Some materials have shown that they can be used for the aggregation of pathogens like DNA Aptamer-conjugated magnetic graphene oxide.[7] The use of magnetic nanoparticles as a sensor for the detection of pathogens is a concept that takes advantage of the intrinsic material properties of such particles. The imperative mandate to work with magnetic nanoparticles for pathogen detection is their ability to separate the particles after capturing the pathogens from the media. This basic principle encompasses different approaches, mainly exploiting specific host–target interactions.[8,9] In recent years, due to the rapidly growing field of nanotechnology, there have been a variety of applications for magnetic particles in both science and industry. This applies to the fields of point-of-care testing, biosensing and biomedicine in general. An important, if not the most important factor for making magnetic nanoparticles useful in diagnostics is the binding interface on the surface of these particles interacting with the analyte. In our case, we used a peptide derived from the human protein GP340, also known as "Salivary Agglutinin" (SAG) or "Deleted in Malignant Brain Tumours 1" (DMBT1). GP340, a protein with remarkable pathogen-binding properties, is found eg in human saliva as a humoral component of the innate immune system.[10,11] This protein is a member of the "scavenger receptor cysteine-rich domain" (SRCR) protein family and is present in humans in various body fluids (except blood) where it aggregates various pathogens (intact microorganisms such as bacteria or viruses and their fragments, such as lipopolysaccharide, LPS, or lipoteichoic acid, LTA).[12,13] According to latest findings, the target spectrum might be much larger and also covers a wide variety of fungi.[14,15] The reason for this could be that fungal cell wall components contain structures that are comparable to LPS and LTA, making its binding to GP340 likely as well.[16,17]

In our study, we investigated previously developed, GP340-peptide-functionalized SPIONs for their capacity to extract *Candida albicans* from different media under static and flow conditions. This was accompanied by theoretical simulations. Moreover, we investigated the feasibility to regrow the extracted fungal cells on culture plates and checked relevant interactions of the functionalized nanoparticles with different host cells.

Materials and Methods

Materials

Most chemicals used in this study, such as ammonia, 25% (v/v) water solution, (3-aminoprpyl)triethoxysilane (APTES, ≥ 98%), N,N-Dimethylformamide (DMF, ≥ 99.5%) hydrochloric acid concentrated, nitric acid, sodium hydroxide, glutaraldehyde 25% (for microscopy) in phosphate buffer, ethanol (absolute), acetone (100% anhydrous), hardener MNA, DPA glycidyl ether (100%), accelerator DMP 30, NaOH (1 M), hydrochloric acid 1N, potassium bromide (KBr) (spectroscopy grade), dimethyl sulfoxide (DMSO, 99.5%) and boric acid, were purchased from Carl Roth GmbH + Co, KG, Germany. N-succinimidyl bromoacetate was supplied by VWR International GmbH, Germany. Ringer's solution was obtained from Fresenius Kabi (Bad Homburg, Germany). RPMI 1640 medium supplemented with 10% fetal calf serum (FCS) and 1% L-glutamine was obtained from Live Technologies (Carlsbad, CA, USA). Science Service (Munich, Germany) supplied OsO_4, copper grid. Merck (Darmstadt, Germany) supplied $K_3(Fe(Cn)_6)$, agarose (low melting point), lead(II)citrate-3-hydrate as well as Iron(II) chloride tetrahydrate, iron(III) chloride hexahydrate. Serva (Heidelberg, Germany) supplied uranyl acetate iron(II) chloride tetrahydrate, while iron(III) chloride hexahydrate and bovine serum albumin lyophilized powder were purchased from Merck KGaA, Germany. Propidium iodide (PI, 94%) and Triton X-100 were purchased from Sigma-Aldrich (Taufkirchen, Germany), and fetal calf serum (FCS) was obtained from Biochrom (Berlin, Germany).

The peptides Pep (RKQGRVEVLYRASWGTVC) and antibPep (RKQGRAEALYRASWGTVC) with >85% purity were obtained from Proteogenix (Schiltigheim, France). Deionized (di.) water was produced using a Merck Milli-Q purification system. All reagents were used without further purification.

Synthesis and Characterization of SPION-APTES-Pep

SPION-APTES were produced by alkaline precipitation as described in [18,19]. Briefly, Iron(II) chloride tetrahydrate and iron(III) chloride hexahydrate were dissolved in di. water.[19] Precipitation was initiated by the addition of ammonia 25% (v/v) at 90 °C followed by stirring for 15 min before the addition of APTES and an additional stirring for 3 h at 70 °C. Particles were washed three times and re-dispersed with di. water and stored at 4 °C until further use. For control, SPIONs without coating were produced by the same synthesis route but omitting the addition of APTES. For functionalization, borate buffer 0.05 M at a pH of 8.5 was used for the next steps. The iron concentration during processing was adjusted to 1 mg Fe/mL together with an amount of 20 mM N-succinimidyl bromoacetate (SBA) dissolved in dimethylformamide (DMF). The functionalization was carried out on a shaker for 2 h at 1400 rpm at room temperature. After that, the particles were washed several times with buffer. The obtained SBA-functionalized particles were redispersed in the corresponding buffer with peptides at a concentration of 0.1 µmol/mL per 1.0 mg Fe/mL. The dispersion was again incubated on a shaker for 2 h at 1400 rpm at RT. The final functionalized SPION-APTES-Pep were magnetically collected and washed with buffer and deionized water. The resulting supernatants were collected and analyzed at 280 nm to determine the amount of peptide on the particles using the LIBRA S22 spectrophotometer (Biochrom Ltd., Cambridge, United Kingdom), as described previously.[18,19]

General characterization of the particles concerning iron content, hydrodynamic size, ζ-potential magnetic susceptibility and Fourier transform infrared spectroscopy (FTIR) were performed according to recently described methods.[19] The final SPION-APTES-Pep were redispersed in di. water or Ringer's solution and stored at 4 °C until further use. For the investigation of the surface chemistry, the samples were characterized with FTIR. SPIONs that were prepared by freeze-drying (Alpha 1–2 LD plus, Martin Christ, Osterode am Harz, Germany) were used in 1% (wt/wt) with potassium bromide (for measurements of KBr pellets) or freeze-dried samples (for attenuated total reflectance (atr) measurements) were analyzed using the FTIR spectrometer (Alpha-P, Bruker, Billerica, United States) with an atr or KBr unit. The OPUS software version 7.2.139,1294 (Bruker, Billerica, United States) was used for the subtraction of background signals as well as baseline correction.

Preparation of Blood for Experiments

For the experiments, freshly drawn peripheral blood from healthy donors was anticoagulated by tri-sodium citrate and used after written informed consent had been obtained. The use of human blood in this study was approved by the ethics committee of the Friedrich-Alexander Universität Erlangen-Nürnberg (license number 346_18B, 343_18B, 357_19B, 257_14 B) and the donors provided informed consent in accordance with the Declaration of Helsinki.

Culturing of *Candida albicans*

Candida albicans isolate (SC ADH AG4A #1509) was grown in liquid Sabouraud media overnight at 37 °C. For re-culturing purposes, Sabouraud agar (SAB) containing 10 g/L peptone, 40 g/L glucose and 15 g/L agar in ~900 mL of deionized water was prepared with the pH adjusted to 5.6 by hydrochloric acid and a final volume of 1 litre. The media was autoclaved 20 minutes at 121 °C, 15 lb/in^2.

Removal of Candida Cells from Different Media and Regrowth After Separation

Candida albicans overnight cultures were centrifuged with 400 rcf for 5 min and washed with Ringer's solution before further use. In general, Ringer's solution was used as dispersion media for static and dynamic separation experiments. The amount of *Candida albicans* for these experiments was set to an OD_{600} of 1.0 (final value after addition of particles or controls). For static separation, the yeast (final OD 1.0) was separated in a total volume of 1 mL with 100 and 300 µg Fe/mL of SPION-APTES-Pep or SPION-APTES-antibPep after 5 min of incubation at 700 rpm on a shaker, followed by magnetic separation of 3 min (using neodymium magnet ~210 mT). Similarly, the same particle concentrations were used

for samples incubated under flow conditions for 5 min at 37 °C or by 700 rpm on a shaker, followed by magnetic separation of 3 min (using neodymium magnet ~210 mT). Particles were re-dispersed in 1 mL Ringer's solution and 50 µL were spread out on Sabouraud agar plates and incubated at cell culture conditions at 37 °C for 24 h.

For flow experiments with *Candida albicans*, a peristaltic pump G100-1J (Longer Precision Pump Co., Baoding, China), tubes and chamber from MIVO® platforms supplied by React4Life (Genova, Italy) were used. A volume of 3 mL of the solution was circulating at 10 mL/min in the device. SPION-APTES-Pep or SPION-APTES-antibPep to reach a final concentration of 100 and 300 µg Fe/mL (final volume) or Ringer's solution as negative control were added. The resulting dispersion of particles and yeast was incubated under flow conditions for 5 min, followed by the addition of a magnet below the camber of the MIVO® system. The magnetic separation was carried out for 3 minutes at a constant flow of 10 mL/min.

After magnetic separation, supernatants were collected and analyzed at OD_{600}. After static separation, microscopic images were taken using the AXIO Observer Z1 inverted fluorescence microscope (Zeiss, Oberkochen, Germany) with extinction/emission 450–490/515–565 filters.

For experiments in citrate-stabilized blood, highly diluted yeast suspensions up to ~ 10^3 CFU/mL were used. Separation was carried out according to previous experiments with 5 minutes of incubation at 37 °C followed by 3 minutes of magnetic separation (as described before). Separated particles were redispersed in Ringer's solution. The supernatants and SPION-APTES-Pep with bound yeast were plated out on Sabouraud-agar plates and incubated at cell culture conditions at 37 °C for 24 h.

To show the regrowth of *Candida albicans* after binding to SPION-APTES-Pep, samples from separation of *Candida albicans* carried out in citrate-stabilized blood with about 10^3 CFU/mL were used. SPION-APTES-Pep, *Candida albicans*-spiked blood samples before and after separation, as well as SPION-APTES-Pep after separation were examined. In addition, and controls without blood were carried out for medium (alone) and yeast in medium 10^3 CFU/mL. Samples were spiked by adding 5 µL of each sample into 195 µL of Sabouraud-media in a 96-well plate. A gas-transparent sealing film was used to cover the plate before it was placed in the SpectraMax iD3 Plate reader (Molecular Devices, San José, USA), where it was shaken at moderate speed and at a temperature of 37 °C. Optical densities of the wells were monitored at 600 nm every 30 minutes for 24 h.

Thermogravimetric Analysis (TGA) Analysis

TGA analysis was performed for a selection of SPIONs without functionalization, SPION-APTES, SPION-APTES-Pep and the peptide (Pep). The analysis was carried out under an N_2 atmosphere from room temperature (35°C) to 1000 °C using a TGA (TG 209 F1 Libra, Netzsch) instrument to define the amount of peptide on the particles.

Storage Stability

To initially evaluate the storage stability of SPION-APTES-Pep particles were stored at 4 °C for 12 weeks in water. Particles were tested directly after functionalization and after 12 weeks for changes in their hydrodynamic size, ζ-potential and susceptibility, UV-Vis and FTIR spectra.

SPION Influence on the Cell Cycle of Different Human Blood Cells

For the toxicological evaluation of SPION-APTES-Pep, Jurkat cells (ACC 282 purchased from DSMZ) and THP-1 cells (ACC 16 purchased from DSMZ) were used along with PBMCs that had been isolated from Li-heparin-stabilized blood, using Vacutainer CPT Tubes after centrifugation for 20 min at 1695 g at RT.[19] Jurkat and THP-1 cells were passaged twice a week. Jurkat cells and PBMCs were cultured in RPMI-1640 medium, supplemented with 10% FCS and 1% L-glutamine at 37 °C and humidified 5% CO_2 atmosphere. THP-1 cells were cultured in the same medium, but with the addition of 1% penicillin/streptomycin. To evaluate the number of cells for the experiments, the MUSE Cell Analyzer was used. Cells were adjusted to a density of 36.000 cells/well and incubated for 24 h with different iron concentrations (50, 200 and 400 µg Fe/mL) of SPION-APTES-Pep. H_2O and DMSO 3% served as controls. Cell cycle and DNA degradation of the different cell types were studied using 50 µL aliquots after 24 h of incubation. Samples were mixed with 250 µL of PIT solution (1 mg/mL sodium citrate, 0.1% (v/v) Triton X-100, and 50 µg/mL PI in water) and incubated

in the dark at 4 °C for 24 h.[20] Samples were analysed by flow cytometry (Gallios, Beckman Coulter, Brea, USA), and data were analysed with the Kaluza software version 2.0 (Gallios, Brea, USA).

For further evaluation of interactions between PBMCs and SPION-APTES-Pep particles (incubations with 300 µg Fe/mL), transmission electron microscopy (TEM) was carried out using the TEM Leo 906 (at 60 keV) with the TRS Tröndle (Moorenweis, Germany) CCD camera and the ImageSP SysPROG software. For preparation, also an Emerson (Saint Louis Missouri, United States) Branson 1200 ultrasonic machine and the Leica (Wetzlar, Germany) Ultracut UCT, Zeiss (Oberkochen, Germany) were used.

Computational Fluid Dynamic and Magnetohydrodynamic Simulations

Computational fluid dynamic and magnetohydrodynamic simulations were performed in COMSOL Multiphysics®, version 6.0, to investigate and predict the flow velocity profiles within the Single-Flow MIVO® device, the fluid flow-driven SPION cell trajectories and the magnetic field caused by a permanent magnet. Likewise, the finite element simulations were done to determine the influence of the fluid flow and the magnetic field on the behaviour of the SPION particles in the filtration chamber. Using the MIVO® chamber geometry, Computational Fluid Dynamics (CFD) simulations were performed. This analysis implies the use of a Single-Phase Laminar Fluid Flow regime, presuming that the media is an incompressible Newtonian fluid with a value of Reynolds number under 2100.[21] Solving the Navier–Stokes equations showed the velocity range from 0 to 0.07 m/s at an imposed inlet flow rate of 10 mm/min (1.67*10e-7 m^3/s). Other parameters and phenomena considered were fluid density ρ (1039 kg/m^3), dynamic viscosity µ (1.08*10-3 PA·s), temperature T (310.15 K), no slip boundary condition for walls and gravity. To determine and obtain a graphic representation of the magnetic field exerted by a permanent magnet, the module Magnetic fields, no currents (mfnc) from Comsol Multiphysics®, was used. The magnetic flux conservation branch was used to define the magnetisation model inside the chamber and in the environment that surrounds the system. This set a linear relationship between the magnetic flux density B, the magnetic field strength H and relative permeability of a medium ($B = \mu_0 * \mu r * H$). For the outside of the defined environment, the Magnetic Isolation feature was used, which set the normal component of the magnetic flux density to 0. For the neodymium magnetic disc, a magnetization M ($B = \mu_0 * (H+M)$) value of 275 mT (218.83 kA/m) was used along the Z axis of the disc.

Statistical Analysis

For statistical analysis, one-way ANOVA, Mann–Whitney or Kruskal–Wallis tests as appropriate were employed to determine statistical significance. P values above 0.05 were considered significant. All statistical analyses were performed using GraphPad Prism 9.0.2.

Results

Characterisation of Peptide Binding to SPION-APTES

As presented in previous studies,[18,19] the obtained nanoparticles with maghemite/magnetite cores had a z-average of about 1.8 µm ± 120 nm with a relatively broad particle size distribution (PDI: 0.3), a positive ζ- potential of around 27.8 mV ± 0.5 mV, and showed a loading of peptide of about 0.094 ± 0.004 µmol/mg Fe, as also demonstrated for different peptides attached to SPION-APTES. The magnetic susceptibility of the functionalized particles was $3.49.10^{-3}$ ± $0.27.10^{-3}$ at a concentration of 1 mg Fe/mL as shown before. Particles were functionalized and used for separation according to Figure 1A. The separation of the yeasts was carried out by incubating the samples with SPION-APTES-Pep for five minutes followed by a three-minute separation. Afterwards, the supernatants were analysed as well as the separated SPIONs.

To further study the peptide and organic content (peptide and APTES) (as the peptide amount on the SPIONs was determined via supernatant analysis after separation), TGA analysis was performed to assess the organic content of the SPIONs and the amount of remaining material after heating the peptide to 1000 °C (Figure 1B). As found in other studies,[22–25] SPIONs without any further functionalisation or coating as well as SPION-APTES showed a similar progression. The TGA curve of the SPIONs show the first weight losses below 200 °C, which is contributed to the

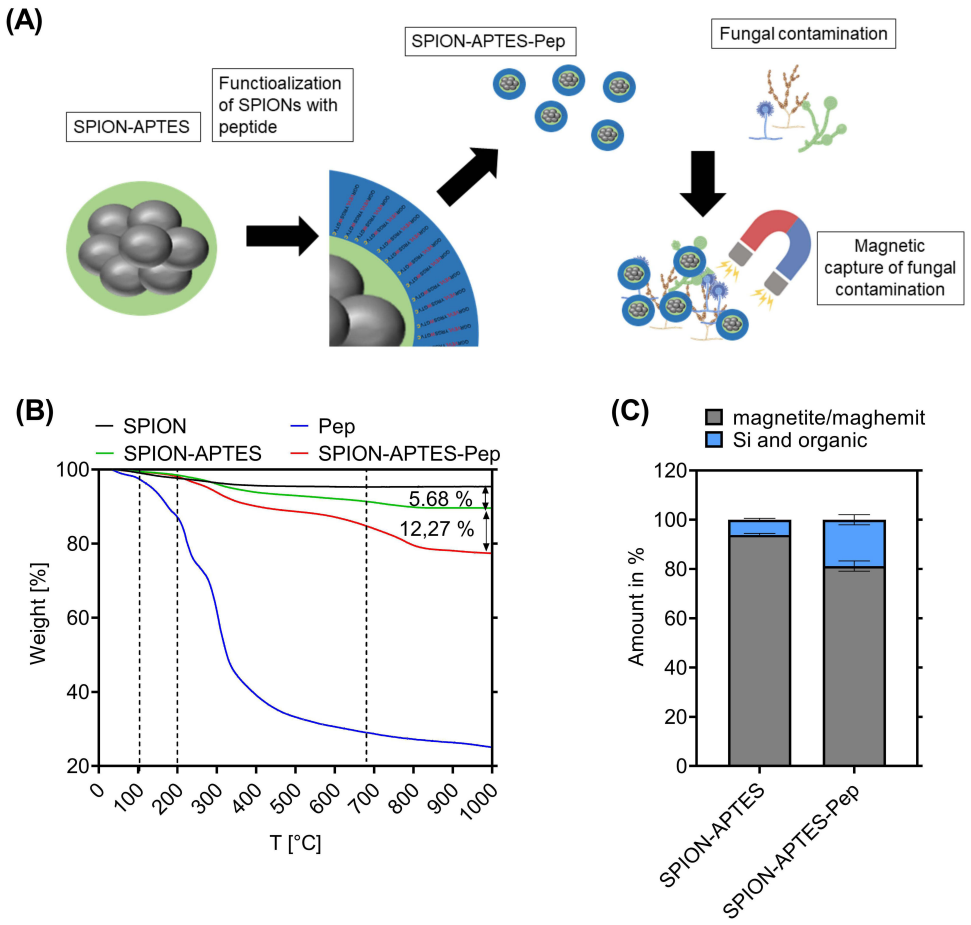

Figure 1 Functionalization of SPION-APTES, use and content of peptide and organic components. (**A**) Functionalization and separation procedure. (**B**) TGA of SPIONs, SPION-APTES and SPION-APTES-Pep and peptide alone. (**C**) Iron oxide and organic content ratio in % (w/w) for SPION-APTES-Pep (iron content was determined after evaporation by AES measurements). Experiments were performed in triplicates. Shown are the mean values with standard deviations.

evaporation of adsorbed water on the nanoparticles with an amount of about 2% to a final amount of weight of 4.5% after reaching 200°C. Between 200 °C and 300 °C, minimal weight loss was observed for SPIONs without functionalisation. After that, the weight is constant up to 1000 °C. For SPION-APTES and SPION-APTES-Pep the weight decreased corresponding to the loss of organic components on that particles. After reaching a temperature of about 680 °C, further weight loss was seen in both these particle types, which was partially attributed to the thermal decomposition of silane.[25] Compared to the unfunctionalized SPIONs, the amount of organic content found on SPION-APTES was 5.68%. The 12.27% weight difference between SPION-APTES and SPION-APTES-Pep represented the quantity of peptide and linker that were decomposed starting at about 200 °C. The TGA curve of the peptide showed a very different progression as for the particles. It can be assumed that water was evaporated till 100 °C. At higher temperatures between 100 °C and about 360 °C, the decomposition of the peptide started with a drastic drop. The following decomposition up to a temperature of 1000 °C was slower and a remaining weight of about 25% of the peptide was found after the measurement (mainly remaining carbon). It was assumed that the peptide present on SPION-APTES-Pep was decomposed slower, as the surface and volume during heating was different for the bare peptide compared to SPION-bound peptide. The solid content was determined by weight measurements after water evaporation in samples with an iron concentration of 10 mg/mL, as shown in Figure 1C, to further evaluate the amount of the magnetite/maghemite organic content on SPION-APTES and SPION-APTES-Pep. As previously described, the particles consisted of a mixture of magnetite/maghemite and the amount of Si was constant and small, compared to the other organic components. The Si/organic content of SPION-APTES was 6.16% ± 0.55% when compared to SPION-APTES-Pep with a content of 18.8% ± 1.88%, which indicates a 13.7% difference in organic content and is thereby relatively close to the values obtained by

TGA as well as the values obtained by peptide quantification after functionalization by UV measurements. To evaluate the surface composition of different SPIONs, FTIR analyses were conducted. The Fourier transform infrared (FTIR) spectra of unfunctionalized SPIONs, SPION-APTES and SPION-APTES-Pep is presented in Figure 2A. The strongest observed peak for all investigated SPIONs is the Fe-O stretching band at around 536 cm^{-1},[26–28] contributing to iron oxide cores of the nanoparticles. For SPION-APTES and SPION-APTES-Pep, bands at 942 and 1090 cm^{-1} correspond to Si-OH and Si-O-Si[22,29–31] due to the functionalization of the SPIONs with APTES. For SPION-APTES and SPION-APTES -Pep as well as for the peptide (Figure 2B), peaks at around 1400 cm^{-1} are present due to CH_2 as well as C-OH deformations. In addition, also C-H vibrant modes are visible in the range of 1200 to 1500 cm^{-1}. For all samples, -OH stretchings and deformation modes were found in the range of 1600 cm^{-1} to 3400 cm^{-1} that are contributed to physically adsorbed water on the SPION surface. The peptide (Figure 2B) showed characteristic aromatic C=C stretchings at 1660 cm^{-1} that are contributed to the amount of aromatic amino acids like tryptophan.[32]

Further also peaks around 1590 cm^{-1} and 1650 cm^{-1} can be found and related to the antisymmetric stretch modes of C=O.[31] Also, C-N stretching was visible for SPION-APTES, SPION-APTES-Pep and peptide at around 1200 cm^{-1}.[31] The changes in the FTIR spectra of SPION-APTES-Pep to SPION-APTES can be described by the linkage of the peptide to the particles as the peaks that contribute to the peptide can be found in the spectra of SPION-APTES-Pep and thereby indicate a successful linkage.

Storage Stability of SPION-APTES-Pep

For any applications, the storage stability is a critical factor for nanoparticles. SPION properties can change over time, even under favourable storage conditions like at 4°C. Therefore, an initial testing of the storage stability was done for a time period of 12 weeks. The properties of SPION-APTES-Pep were investigated directly after preparation and after twelve weeks of storage at 4 °C (Figure 3). Usually, a shift in the colour of a SPION dispersion from black to stronger brown-reddish would be considered as a clear sign of particle oxidation and, therefore, to affect nanoparticle properties. As shown in Figure 3A, no obvious changes were observed between SPION APTES-Pep freshly prepared and particles that were stored for 12 weeks despite the fact that no additional inert gas like nitrogen or argon was added to the storage tubes to prevent oxidation by normal air oxygen.

To evaluate the changes of SPION-APTES-Pep after 12 weeks of storage, an FTIR of dried particles (Figure 3B) was recorded, showing no time-dependent alterations (no changes in the spectra compared to Figure 2). It was observed that in water-based media after 12 weeks, signs of sedimentation occurred. This is contributed to the size of SPION-APTES-Pep, so that gravitational forces cause the sedimentation. However, after vortexing this could be overcome and did not affect the usability. A UV-Vis spectrum, recorded to quantify changes like large aggregation, showed no evidence of decreased or increased intensity at the wavelength tested. As shown previously, the X-ray diffraction (XRD) and selected

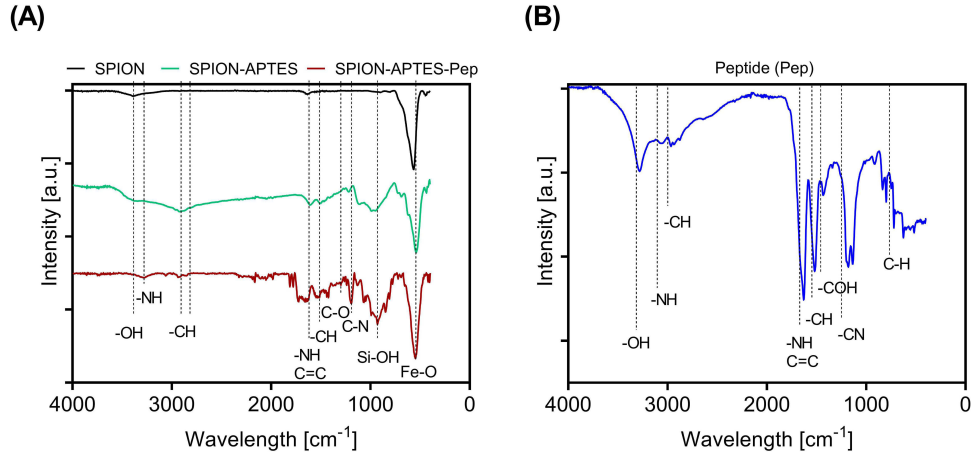

Figure 2 FTIR analysis of (**A**) SPION without coating, SPION-APTES and SPION-APTES-Pep. (**B**) Peptide (Pep).

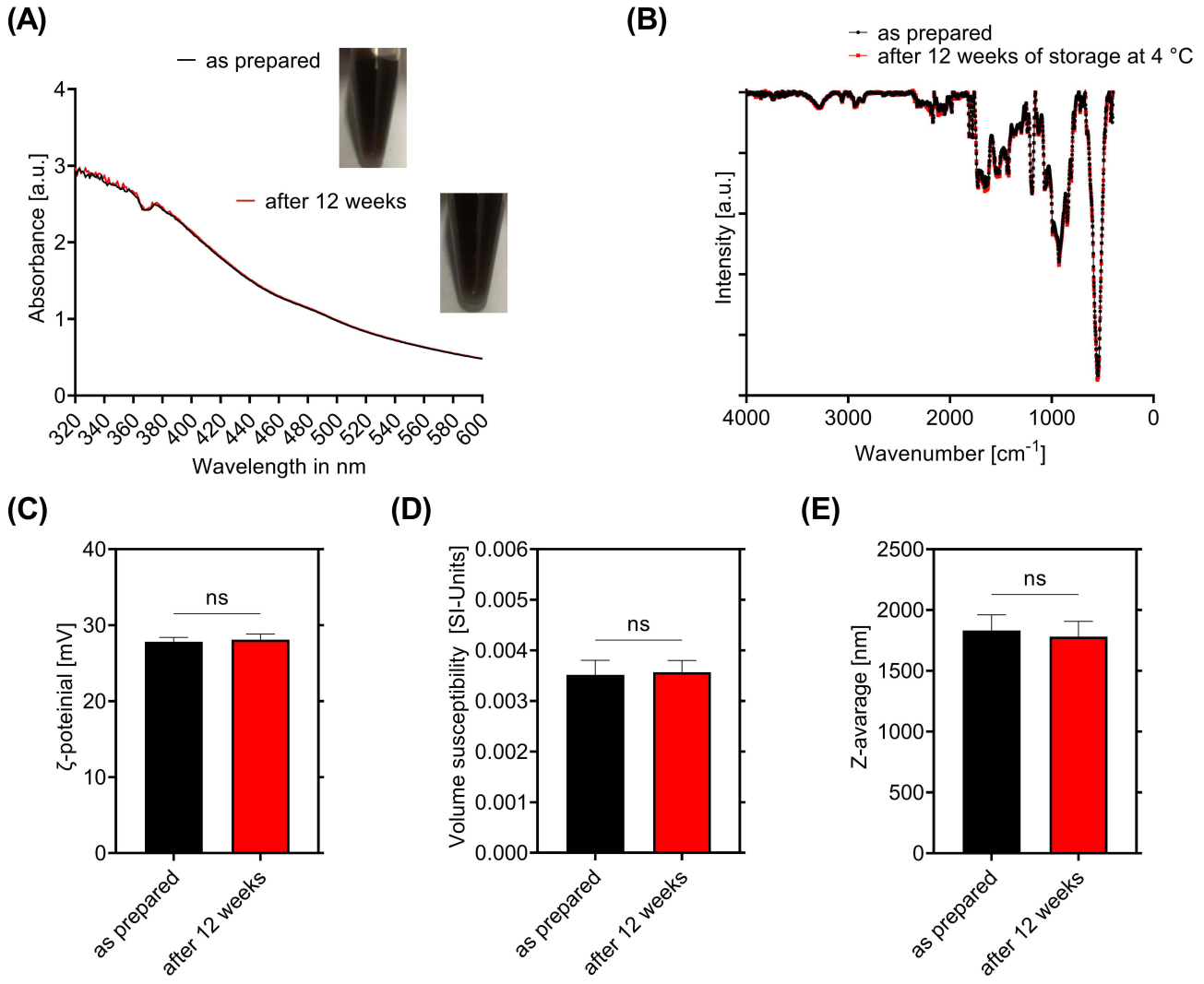

Figure 3 SPION-APTES-Pep after 12 weeks of storage. (**A**) Visual evaluation and UV-VIS spectra of SPION-APTES-Pep (100 µg Fe/mL). (**B**) FTIR measurements (kbr), (**C**) ζ-potential, (**D**) volume susceptibility and (**E**) Z-average of SPION-APTES-Pep freshly prepared and after 12 weeks of storage at 4 °C. Experiments were performed in triplicates. Shown are the mean results with standard deviation. Significance was calculated with a Mann–Whitney *U*-test. P values higher than 0.05 were considered non-significant (ns).

area (electron) diffraction (SAED) analysis showed that SPION-APTES-Pep consists of magnetite/maghemite.[19] This points to the fact that the iron oxide of the particles was already oxidised during synthesis, shielding the inner particle cores from further oxidation.

Further, the ζ-potential, volume susceptibility and hydrodynamic size (Figure 3C–E) showed no significant changes before and after storage. Also, no changes were observed in the pH (7.4) that could influence size or ζ-potential during storage of the particles. Further, the supernatant (after magnetic separation of stored samples) was checked by UV measurements at 280 nm for released peptide over time with no detectable release of peptide from the particles showing a very stable binding of the peptides on the surface of SPION-APTES-Pep.

Evaluation of Changes in Cell Cycle of Different Blood Cells by SPION-APTES-Pep

The cell cycle is a sequence of different phases, such as mitosis (M includes the cytokinesis), gap-phase 1 (G1), synthesis (S) and gap-phase 2 (G2), which is also known as interphase[33] in most eukaryotic cells that are viable and proliferating. The DNA content of the single cell varies in the different stages of the cell cycle. Experimentally, the DNA changes during cell cycle and DNA degradation can be analysed using a PIT staining followed by flow cytometric analysis.[20,34]

An increase in the number of cells in the sub G1 phase is attributed to the death of cells, as DNA is degraded by DNases into smaller fragments during apoptosis (expressed as sub G1-phase) and is therefore another indicator of toxicity.[20,34]

As shown in Figure 4, the cell cycle was analysed in Jurkat T cells, THP-1 cells and PBMCs, freshly isolated from donor blood, after incubation with SPION-APTES-Pep for 24 h. For the treatment with 3% DMSO, a drastic increase in sub G1 phase after 24 h of incubation was observed. No changes in the amounts of cells in the respective cell cycle phases or amounts of degraded DNA were found for SPION-APTES-Pep-treated samples compared to H_2O after incubation 24 h. Thus, the particles are non-toxic at the tested concentrations of 50 to 400 µg Fe/mL. The TEM evaluation of PBMCs as depicted in Figure 4D shows that particles interact with the membranes of PBMCs and are also engulfed by them (red arrow), which, however, does not result in increased toxicity. The amount of viable cells were in agreement with previously observed results of AxV/PI and Dil stainings.[19]

Removal and Regrowth of *Candida albicans* Using SPION-APTES-Pep

The testing of the magnetic removability of *Candida albicans* from media was carried out based on recent protocols developed for bacterial separation experiments with SPION-APTES-Pep. Tests were conducted in a controlled volume under static (no flow, just incubation) conditions and under a constant flow in a tube system, as previously used for bacterial separation (10 mL/min).[18] For the experiments (static and flow conditions), the optical density of the *Candida albicans* suspension (OD_{600}) was adjusted to 1.0 to evaluate the amount of separated yeasts. The results for separation experiments using 100 µg Fe/mL and 300 µg Fe/mL of SPION-APTES-Pep and SPION-APTES-antibPep are shown in Figure 5. High removal efficiencies were observed for both concentrations of SPION-APTES-Pep under static conditions. At a concentration of 100 µg Fe/mL, about 59% of *Candida albicans* cells were removed and even 82% at

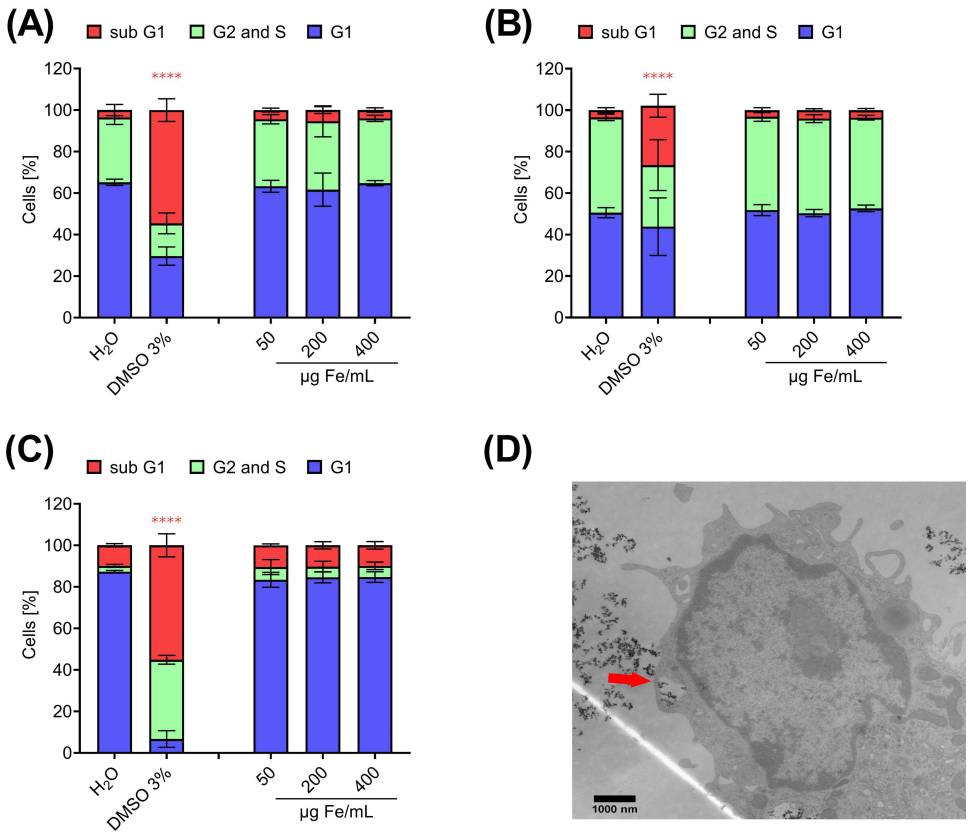

Figure 4 PIT-Analysis of cell cycle phases in (**A**) Jurkat T-cells, (**B**) THP-1 cells and (**C**) PBMCs after incubation with nanoparticles for 24 h. H2O served as negative control and DMSO 3% as positive control. Experiments were performed in three independent replications. Shown are the mean values with standard deviations. Significance was calculated with a one-way ANOVA test; ****p < 0.0001. P values higher than 0.05 were considered non-significant (ns). (**D**) shows a TEM-image of SPION-APTES-Pep engulfed by a phagocytic PBMC (red arrow) after 24 h of incubation with 400 µg Fe/mL.

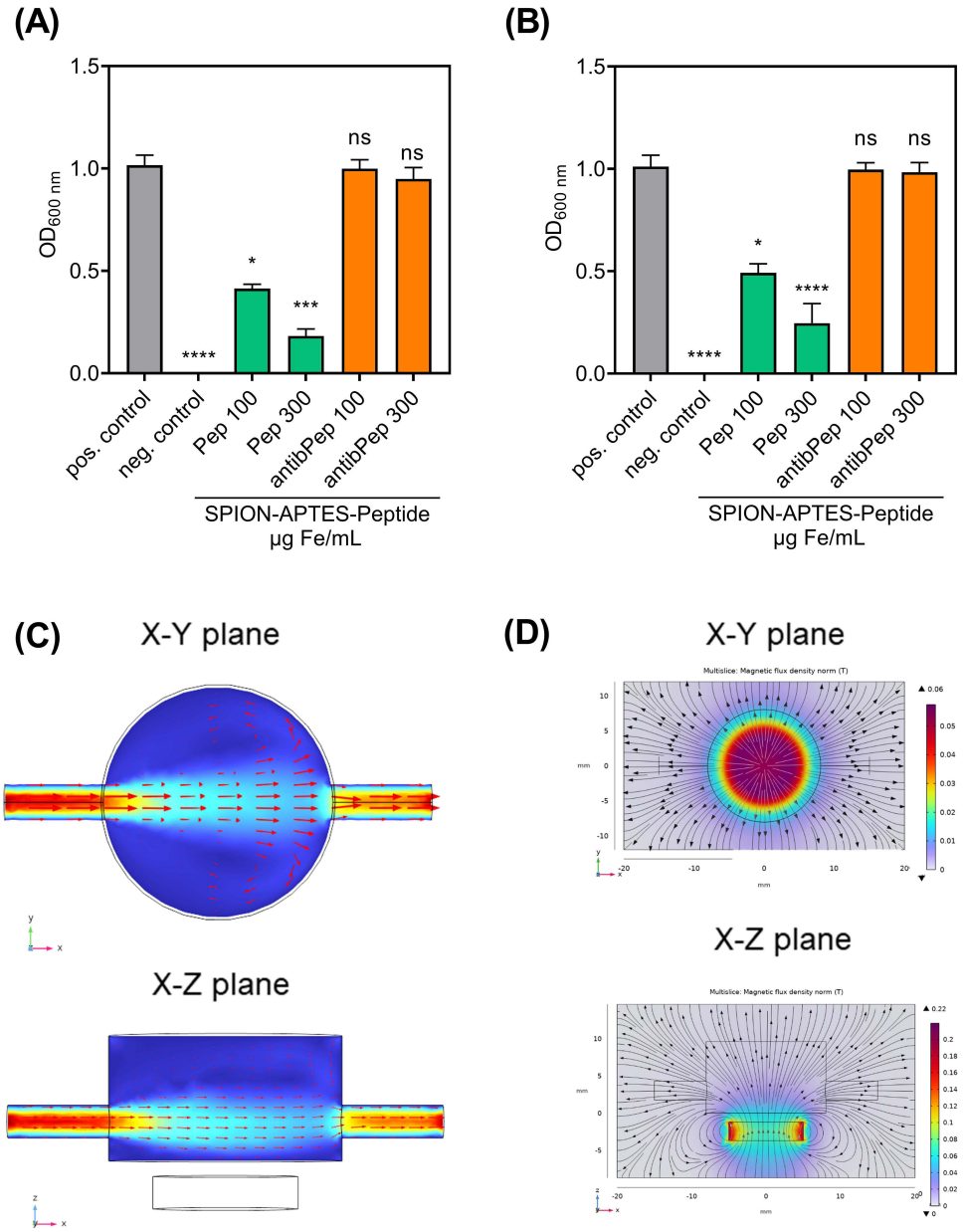

Figure 5 Removal of *Candida albicans* from aqueous (Ringer`s solution) samples. (**A**) Static system and (**B**) dynamic system with a flow rate of 10 mL/min using SPION-APTES-Pep. Different iron concentrations (300 µg Fe/mL and 100 µg Fe/mL) were tested. Untreated *Candida albicans* spiked samples served as positive control and medium without yeast as negative control. SPION-APTES-antibPep served as an additional control. Optical density was measured at 600 nm. Experiments were performed in triplicates of three independent repetitions. Shown are the mean values with standard deviation. Significance was calculated between treatment positive control and samples. Significances were calculated with a Kruskal–Wallis test; *p ≤ 0.05; ***p ≤ 0.001; ****p < 0.0001. P values higher than 0.05 were considered non-significant (ns). Simulation of the flow in the mix/separation camber (**C** and **D**) the magnetic flux density.

a concentration of 300 µg Fe/mL (Figures 4A). Surprisingly, the removal efficiency under flow conditions was in the same range for both particle concentrations. Under a flow rate of 10 mL/min 50% of cells were removed by SPION-APTES-Pep at 100 Fe µg/mL, and 76% at 300 µg Fe/mL (Figure 4B). SPION-APTES functionalized with an anti-binding peptide (antibPep) did not remove any significant amounts of *Candida albicans* even at any concentration tested (Figure 5A and B). For a theoretical understanding of the separation under flow conditions, simulations were performed. They showed that the highest flow was found at the connections of the chamber and in the middle of it (Figure 5C). As gravitation will also drive *Candida albicans* to this direction, this led to a good mixing of the media/dispersion.

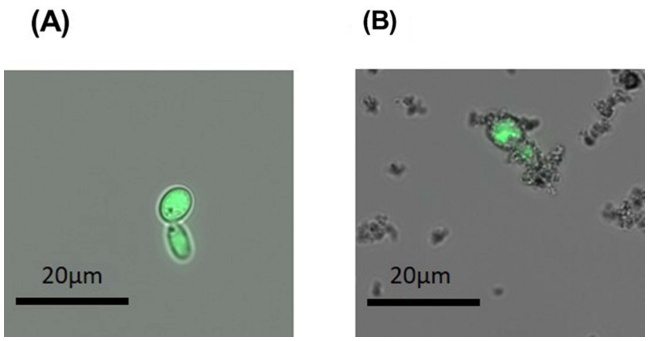

Figure 6 (**A**) Separation of *Candida albicans* (fluorescent strain) under static conditions in water-based media (Ringer`s solution). Before separation the cells are without any attachment at the cell wall. (**B**) After separation with SPION-APTES-Pep *C. albicans* cells from the magnetic pellet show attachment of particle clusters to the wall of the cells.

According to the simulation, the maximum of the magnetic flux density is located directly in the centre of the magnet and SPION-APTES-Pep is expected to be driven to this area (seen in Figure 5D). Also, gravity force enhances the movement of the particle towards the bottom of the filtration chamber, resulting in a magnetic accumulation above the magnet.[35] This is in good accord with the experimentally observed results.

Figure 6 shows unseparated *Candida albicans* (A) and images of with SPION-APTES-Pep removed *Candida albicans* after separation in water-based media (6 B). It was found that the particles form a corona around the cells of *Candida albicans*, showing a strong interaction between cells and particles.

Figure 7 represents the evaluation of the separation efficiency of yeast out of citrate-stabilized blood. The amount of *Candida albicans* was set to about 10^3 CFU/mL for these experiments. Separation experiments were carried out using

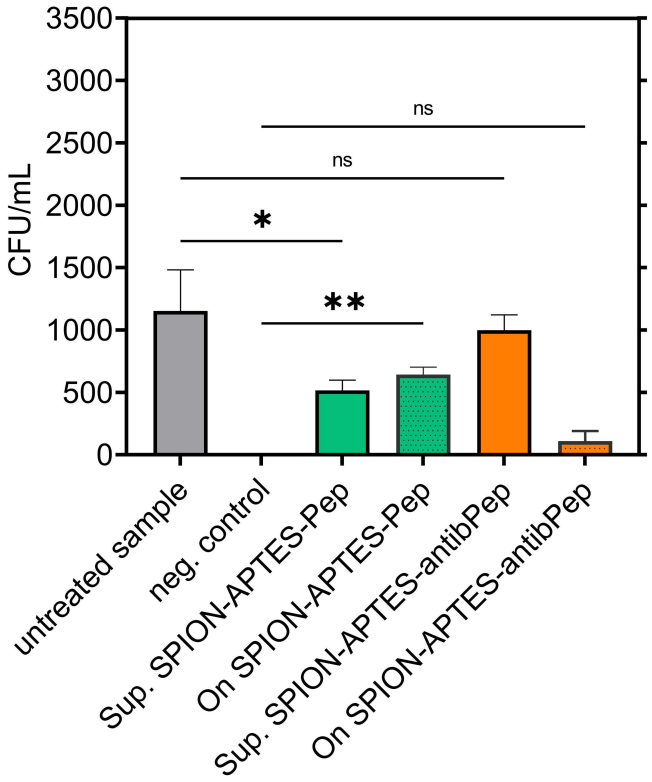

Figure 7 Removal and reculture of *Candida albicans* using SPION-APTES-Pep and SPION-APTES-antibPep. For the removal, the initial amount of *Candida albicans* in citrate-stabilized blood was set to a number of about 103 CFU/ mL. Experiments were performed in triplicates of three independent repetitions. Shown are the mean values with standard deviations. Significances were calculated between untreated samples with *Candida albicans* and treatment groups at the respective time. Significance was calculated with a Kruskal–Wallis test; *p ≤ 0.05; **p ≤ 0.001. P values higher than 0.05 were considered non-significant (ns).

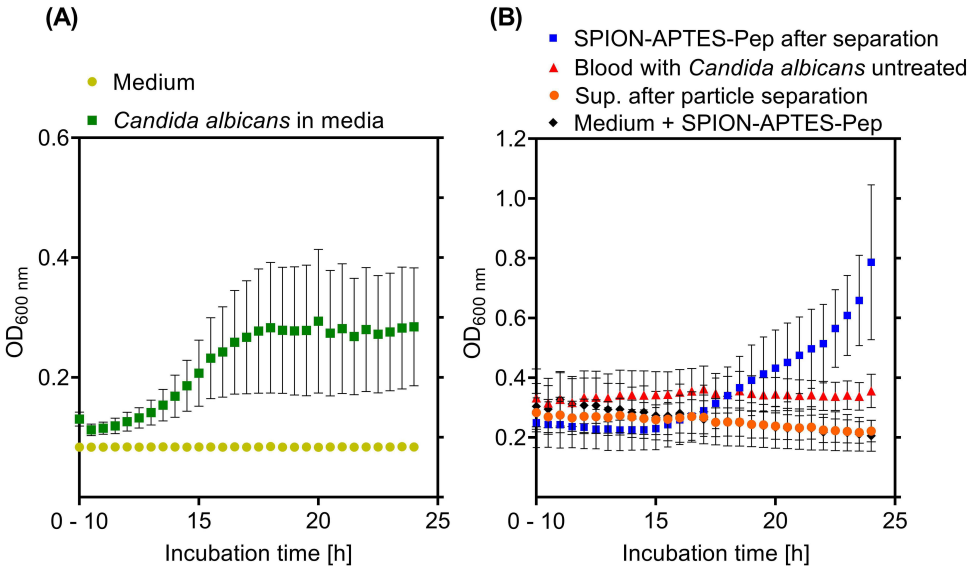

Figure 8 Growth and regrowth of *Candida albicans*. (**A**) Initial amount (before spiking into the culture medium) of *Candida albicans* was set to about 103 CFU/ mL. Samples were incubated for 24 h in culture medium. (**B**) Supernatant and SPION-APTES-Pep (in Ringer´s solution) after separation from citrate-stabilized blood were incubated in media (initial amount of candida was set to 103 CFU/ mL). Media with SPION-APTES-Pep and spiked blood samples are also shown. Samples were incubated for 24 h. Shown are the mean values from 10 h to 24 h of incubation with standard deviations.

300 µg Fe/mL of particles. Afterwards, SPION-APTES-Pep (with *Candida albicans* bound) were redispersed in 1 mL and 50 µL were spread out on plates. Then, the number of CFU bound to the particles was determined by redispersng the particles and spreading them 50 µLout on plates. The number of CFU in blood samples incubated with SPION-APTES-Pep was significantly reduced after separation. Around 515 CFU/mL were found in the supernatant, corresponding to a reduction of 55% compared to the untreated sample. In addition, the particle bound yeast was plated out to show that the remaining yeasts that were not found in the supernatant after separation were particle bound.

To further evaluate the regrowth of *Candida albicans* in samples, their growth in medium was observed after spiking 5 µL of a sample, containing an amount of approximately 10^3 CFU/mL, into media (Figure 8A). After 10 h of incubation, a slow increase in optical density was visible, attributable to the growth of the yeast. For media alone, no growth was found, as seen in Figure 8A. In additional experiments, SPION-APTES-Pep, media, supernatant and particles after separation of *Candida albicans* (as performed before, Figure 5 redispersed in Ringer's solution) were spiked into media (Figure 8B). After 18 h of incubation, an increase in optical density was detectable in samples spiked with SPION-APTES-Pep, which were separated after binding *Candida albicans*. The differences in initial optical density and growth between *Candida albicans* in medium (Figure 8A) and the samples with particle-bound yeast (Figure 8B) can be explained by the different sample compositions spiked into the media (the addition of SPIONs and blood increases the optical density).

No changes were found in samples spiked with bare SPION-APTES-Pep, confirming that they were not contaminated. No significant changes were also observed in the untreated blood samples or in the supernatant after separation. This absence of growth observed for these samples can be related to the presence of unspecific antibodies and immune cells in blood.[36,37] The low number of yeasts in these samples slows down the growth in the beginning, but then usually a drastic increase follows, albeit this could not be observed in the present experiments. Yeast cells separated magnetically by SPION-APTES-Pep were washed after the separation step. Thus, the load of potential immune cells and antibodies interacting with the yeast was reduced, making growth of the particle-bound *Candida albicans* possible.

Discussion

Besides bacteria, also fungi/yeasts, and in particular *Candida albicans*, can cause sepsis.[38] The separation of *Candida albicans* by magnetic particles has been achieved before,[39] but without showing its potential for re-culturing and diagnostic use. Several approaches have been developed for the separation of pathogenic micro-organisms. They differ

mainly in the type of interface attached to the particles at which the pathogen is to be separated. Polymyxin B was able to remove relatively high concentrations of endotoxin. However, quantitative elimination was not possible.[40] Genetically modified mannose-binding lectins (MBLs) have been used in extracorporeal blood purification to remove over 90% of gram-positive and gram-negative bacteria and fungi,[39] but the complex genetic engineering required to modify MBLs makes their use difficult. Another approach is to use poly-N-acetylglucosamine as a target, but this could be hampered by the lack of expression of the epitope[41,42]. There is also the possibility of attaching specific antibodies to the surface of the particles, but this would only recognise the desired pathogen, leaving unknown invaders undetected.[43] In this study, we aimed at exploring the potential of superparamagnetic functionalized with a peptide derived from the human protein GP340 to magnetically extract *Candida albicans* from buffer and citrate stabilized blood under static conditions and from buffer under flow conditions. As shown before by our group, this was already known for gram-positive and gram-negative-bacteria and the respective cell wall components lipoteichoic acids (LTA) and lipopolysaccharides (LPS).[18,19,44] So, the question arose, if the GP340-peptides and by that the functionalized particles are also capable of removing fungi and especially *Candida albicans* in the same manor, since this fungus is among the top 10 pathogens causing sepsis in human patients. Nevertheless, there are major differences between fungi and bacteria. One difference is the larger size of *Candida albicans* cells (up to 8 µm), but also the structure of the fungal cell wall differs significantly from that of bacteria.[17,45,46] However, the fungal cell wall possesses structures like glycosylphosphatidylinositol-anchored proteins or phosphomannan, which could be bound by the peptides.[15,17] Additionally, the ζ-potential of *Candida albicans* was found to be slightly negative,[45] and therefore ideal for the interaction with particles that possess a positive ζ-potential.

From the material characterization point of view, we could further confirm the value of particle-bound peptide by evaluating the amount of organic content on the surface of the particles. Considering that the amount of iron was given, the calculated amount of organic content that was determined by TGA and AES measurements fits the 0.094 µmol peptide/mg iron that was measured by UV and is also in good accordance with the results of TGA.

Assessing the toxicological potential of the particles with flow cytometry, the PIT staining further showed that no significant effect could be found on the cell cycle of human white blood cells incubated with SPION-APTES-Pep. The amount of viable and especially dead cells according to the PIT staining was in good agreement to data, previously observed when using AxV/PI and Dil stainings.[19] This demonstrates a good biocompatibility, which is of high relevance if the particles are intended for use in the diagnostic of candida or bacterial induced blood stream infections and especially in sepsis. On the other hand, the excellent biocompatibility is of even much higher importance, if one imagines patients displaying symptoms of sepsis, while having only a very low pathogen load in the blood making positive blood culture and the respective diagnosis extremely difficult or impossible. For these patients one could imagine an in vivo bypass magnetic extraction system similar to a dialysis device to gain a much bigger volume as a blood sample reinfusing the blood to the patient after pathogen and particle extraction.

The results of the separation experiments suggest that peptide-functionalized SPIONs can be used for the removal of *Candida albicans* from blood and for accelerating the corresponding diagnostic procedure to detect fungi/yeasts, for which usually an additional blood culture bottle is required. Due to the large size of *Candida albicans* cells, an agglutination test to evaluate the best peptide useable for the binding could unfortunately not be performed, as the rapid cell sedimentation could only be prevented by agitation. Similar to previous experiments carried out with bacteria,[18] the removal efficiency of yeasts was only slightly decreased under a flow rate of 10 mL/min in comparison to static conditions. It was shown that SPION-APTES linked to the non-binding control peptide sequence RKQGRAEALYRASWGTVC lead to a complete absence of binding to yeast as it had been observed for bacteria before.[18] Similar to experiments with *S. aureus*, SPION-APTES-Pep form a dense corona around the candida cells.[18,19] These observations correspond to the separation efficiency for SPION-APTES-Pep, pointing out an excellent attachment of the particle-bound peptide to the yeast cells. In the recultivation experiments, we could show that *Candida albicans* cells extracted from blood showed much better growth in culture medium than cells from the supernatant or spiked directly in blood. It is known from the literature that the growth from *Candida albicans* is decelerated by unspecific antibodies and immune cells.[36,37] This is one important reason, why in sepsis diagnosis the time to identify *Candida albicans* as the causing pathogen is so time-consuming. The results of our study suggest that peptide-functionalized SPIONs cannot only remove *Candida albicans* from blood, but also accelerate the diagnosis without the need of an additional blood culture bottle to detect fungi.[47]

From the pharmaceutical point of view, one important factor that influences the possibility of a drug or an in vitro diagnostic system is storage stability. To asses first inside in this highly relevant property, we conducted a preliminary study of storage

stability over 12 weeks at 4 °C. Our data show that the standard physio-chemical properties of SPION-APTES-Pep were not affected by these storage conditions over 12 weeks. Nevertheless, above these material parameters, the functionality needs to be proven as well. In this context, a test of the separation efficiency was done to prove that the particles were equally effective after storage, as they were directly after production. In general, the evaluation showed that the general properties are not affected at the tested storage time.

Conclusion

In conclusion, the present work demonstrates that SPION-APTES-Pep are successfully functionalized with used peptides and do not affect the cell cycle of human leukocyte cells. The removal of yeast, here *Candida albicans*, was possible by the use of a very broad binding motif of saliva peptides on functionalized SPION-APTES. Removal and re-growth of the bound yeast was shown and initial assessment of storage stability of the particles was successful. Hence, SPION-APTES-Pep exhibit a high potential to be used for the separation of yeast and other pathogens that can cause bloodstream infections (i.a. sepsis) from blood or other media and also for pathogen identification after re-cultivation.

Abbreviations

di water, deionized water; SPION, superparamagnetic iron oxide nanoparticles; CFU, colony forming units; CFD, computational fluid dynamics.

Data Sharing Statement

The data that support the findings of this study are available from the corresponding author upon reasonable request.

Ethics

The Jurkat T-cells and the THP-1 cells were purchased from the DSMZ.

Acknowledgments

We acknowledge the work of Andrea Hilpert and Anita Hecht from the Institute of Anatomy and Cell Biology, Friedrich-Alexander-Universität Erlangen-Nürnberg (FAU, Erlangen, Germany) for the preparation of samples for TEM-imaging. Professor Joachim Morschhäuser from the Julius-Maximilians-Universität Würzburg, Germany, is thanked for providing the GFP-tagged *Candida albicans* isolate.

Funding

We gratefully acknowledge the generous support by the Manfred Roth-Stiftung, Fürth (Germany), as well as by the Forschungsstiftung Medizin am Universitsätsklinikum Erlangen (Germany) and Hans Wormser, Herzogenaurach (Germany). Moreover, this work was supported by the Deutsche Forschungsgemeinschaft (German Research Foundation), AL 552/20-1, VO 2288/1-1, VO 2288/3-1, and BE 5293/1-2. We acknowledge financial support by Deutsche Forschungsgemeinschaft and Friedrich-Alexander-Universität Erlangen-Nürnberg within the funding programme "Open Access Publication Funding".

Disclosure

Dr Bernhard Friedrich reports a patent EP 20210959.1 pending to Bernhard Friedrich, Rainer Tietze, Stefan Lyer, Christoph Alexiou. Dr Rainer Tietze reports a patent EPA-149 063 pending (application is still under review). Prof. Dr. Stefan Lyer reports a patent EP4009049A1 with royalties paid to Friedrich-Alexander-Universität Erlangen/Nuernberg. The authors report no other conflicts of interest related to this work.

References

1. Delaloye J, Calandra T. Invasive candidiasis as a cause of sepsis in the critically ill patient. *Virulence*. 2014;5(1):161–169. doi:10.4161/viru.26187
2. Jerez Puebla LE. *Fungal Infections in Immunosuppressed Patients*. IntechOpen; 2012:149–176.

3. Ibáñez-Martínez E, Ruiz-Gaitán A, Pemán-García J. Update on the diagnosis of invasive fungal infection. *Rev Esp Quimioter*. 2017;30(Suppl 1):16–21.
4. Herbrecht R, Neuville S, Letscher-Bru V, Natarajan-Amé S, Lortholary O. Fungal infections in patients with neutropenia: challenges in prophylaxis and treatment. *Drugs Aging*. 2000;17(5):339–351. doi:10.2165/00002512-200017050-00002
5. Duggan S, Leonhardt I, Hünniger K, Kurzai O. Host response to Candida albicans bloodstream infection and sepsis. *Virulence*. 2015;6(4):316–326. doi:10.4161/21505594.2014.988096
6. Carolus H, Van Dyck K, Van Dijck P. Candida albicans and Staphylococcus species: a threatening twosome. Mini review. *Front Microbiol*. 2019;10. doi:10.3389/fmicb.2019.02162
7. AOcsoy M, Yusufbeyoglu S, Ildiz N, Ulgen A, Ocsoy I. DNA aptamer-conjugated magnetic graphene oxide for pathogenic bacteria aggregation: selective and enhanced photothermal therapy for effective and rapid killing. *ACS Omega*. 2021;6(31):20637–20643. doi:10.1021/acsomega.1c02832
8. Chu YW, Engebretson DA, Carey JR. Bioconjugated magnetic nanoparticles for the detection of bacteria. *J Biomed Nanotechnol*. 2013;9(12):1951–1961. doi:10.1166/jbn.2013.1701
9. Yu X, Zhong T, Zhang Y, et al. Design, preparation, and application of magnetic nanoparticles for food safety analysis: a review of recent advances. *J Agric Food Chem*. 2022;70(1):46–62. doi:10.1021/acs.jafc.1c03675
10. Fan Y, X-d L, P-p H, et al. A biomimetic peptide recognizes and traps bacteria in vivo as human defensin-6. *Sci Adv*. 2020;6. doi:10.1126/sciadv.aaz4767
11. Leito JT, Ligtenberg AJ, van Houdt M, van den Berg TK, Wouters D. The bacteria binding glycoprotein salivary agglutinin (SAG/gp340) activates complement via the lectin pathway. *Mol Immunol*. 2011;49(1–2):185–190. doi:10.1016/j.molimm.2011.08.010
12. Leito JT, Ligtenberg AJ, Nazmi K, de Blieck-Hogervorst JM, Veerman EC, Nieuw Amerongen AV. A common binding motif for various bacteria of the bacteria-binding peptide SRCRP2 of DMBT1/gp-340/salivary agglutinin. *Biol Chem*. 2008;389(9):1193–1200. doi:10.1515/BC.2008.135
13. Leito JT, Ligtenberg AJ, Nazmi K, Veerman EC. Identification of salivary components that induce transition of hyphae to yeast in Candida albicans. *FEMS Yeast Res*. 2009;9(7):1102–1110. doi:10.1111/j.1567-1364.2009.00575.x
14. Ligtenberg AJ, Karlsson NG, Veerman EC. Deleted in malignant brain tumors-1 protein (DMBT1): a pattern recognition receptor with multiple binding sites. *Int J Mol Sci*. 2010;11(12):5212–5233. doi:10.3390/ijms1112521
15. Murciano C, Moyes DL, Runglall M, et al. Candida albicans cell wall glycosylation may be indirectly required for activation of epithelial cell proinflammatory responses. *Infect Immun*. 2011;79(12):4902–4911. doi:10.1128/IAI.05591-11
16. Reyna-Beltrán E, Bazán C, Iranzo Rodenas M, Mormeneo S, Luna-Arias JP. The cell wall of candida albicans: a proteomics view. *Candida albicans*. 2019;12:71–92.
17. Richard ML, Plaine A. Comprehensive analysis of glycosylphosphatidylinositol-anchored proteins in Candida albicans. *Eukaryot Cell*. 2007;6(2):119–133. doi:10.1128/EC.00297-06
18. Friedrich B, Eichermüller J, Bogdan C, et al. Biomimetic magnetic particles for the removal of gram-positive bacteria and lipoteichoic acid. *Pharmaceutics*. 2022;14(11):2356.
19. Friedrich B, Lyer S, Janko C, et al. Scavenging of bacteria or bacterial products by magnetic particles functionalized with a broad-spectrum pathogen recognition receptor motif offers diagnostic and therapeutic applications. *Acta Biomaterialia*. 2022;141:418–428. doi:10.1016/j.actbio.2022.01.001
20. Riccardi C, Nicoletti I. Analysis of apoptosis by propidium iodide staining and flow cytometry. *Nat Protoc*. 2006;1(3):1458–1461. doi:10.1038/nprot.2006.238
21. Rehm B, Haghshenas A, Paknejad A, Al-Yami A, Hughes J, Schubert J. CHAPTER 2 - flow drilling: underbalance drilling with liquid single-phase systems. In: *Underbalanced Drilling: Limits and Extremes*. Gulf Publishing Company; 2012:39–108.
22. Cao H, He J, Deng L, Gao X. Fabrication of cyclodextrin-functionalized superparamagnetic Fe3O4/amino-silane core–shell nanoparticles via layer-by-layer method. *Appl Surf Sci*. 2009;255(18):7974–7980. doi:10.1016/j.apsusc.2009.04.199
23. Mikhaylova M, Kim DK, Berry C, et al. BSA Immobilization on amine-functionalized superparamagnetic iron oxide nanoparticles. *Chem Mater*. 2004;16(12):2344–2354. doi:10.1021/cm0348904
24. Pourmanouchehri Z, Jafarzadeh M, Kakaei S, Khameneh E. Magnetic nanocarrier containing 68Ga–DTPA complex for targeted delivery of doxorubicin. *J Inorg Organomet Polym Mater*. 2018;28(5):1980–1990. doi:10.1007/s10904-018-0826-7
25. Shen W-Z, Cetinel S, Sharma K, Borujeny ER, Montemagno C. Peptide-functionalized iron oxide magnetic nanoparticle for gold mining. *J Nanopart Res*. 2017;19(2):74. doi:10.1007/s11051-017-3752-7
26. Santos T, Silva M, Andrade M, Vieira M, Bergamasco R. Magnetic coagulant based on Moringa oleifera seeds extract and super paramagnetic nanoparticles: optimization of operational conditions and reuse evaluation. *Desalin Water Treat*. 2018;106:226–237. doi:10.5004/dwt.2018.22065
27. Hwang S, Umar A, Dar GN, Kim S, Badran R. Synthesis and characterization of iron oxide nanoparticles for phenyl hydrazine sensor applications. *Sens Lett*. 2014;12(1):97–101. doi:10.1166/sl.2014.3224
28. Gotić M, Musić S. Mössbauer, FT-IR and FE SEM investigation of iron oxides precipitated from FeSO4 solutions. *J Mol Struct*. 2007;834:445–453. doi:10.1016/j.molstruc.2006.10.059
29. Cornell RM, Schwertmann U. *The Iron Oxide*. Wiley-VCH Verlag; 2003.
30. Acres RG, Ellis AV, Alvino J, et al. Molecular structure of 3-aminopropyltriethoxysilane layers formed on silanol-terminated silicon surfaces. *J Phys Chem C*. 2012;116(10):6289–6297. doi:10.1021/jp212056s
31. Pretsch E, Bühlmann P, Affolter C, et al. *Structure Determination of Organic Compounds*. Springer; 2000.
32. Sadhasivam B, Muthusamy S. Thermal and dielectric properties of newly developed L-Tryptophan-based optically active polyimide and its POSS nanocomposites. *Des Monomers Polym*. 2016;19:1–12. doi:10.1080/15685551.2015.1136530
33. Cooper GM. *The Cell: A Molecular Approach*. 2nd ed. Sinauer Associates; 2000.
34. Nicoletti I, Migliorati G, Pagliacci MC, Grignani F, Riccardi C. A rapid and simple method for measuring thymocyte apoptosis by propidium iodide staining and flow cytometry. *J Immunol Methods*. 1991;139(2):271–279. doi:10.1016/0022-1759(91)90198-o
35. Kappes M, Friedrich B, Pfister F, et al. Superparamagnetic iron oxide nanoparticles for targeted cell seeding: magnetic patterning and magnetic 3D cell culture. *Adv Funct Mater*. 2022:2203672. doi:10.1002/adfm.202203672

36. Ishiguro A, Homma M, Torii S, Tanaka K. Identification of Candida albicans antigens reactive with immunoglobulin E antibody of human sera. *Infect Immun*. 1992;60(4):1550–1557. doi:10.1128/iai.60.4.1550-1557.1992
37. Djeu JY, Blanchard D, Richards AL, Friedman H. Tumor necrosis factor induction by Candida albicans from human natural killer cells and monocytes. *J Immunol*. 1988;141(11):4047–4052. doi:10.4049/jimmunol.141.11.4047
38. Elbaz M, Chikly A, Meilik R, Ben-Ami R. Frequency and clinical features of candida bloodstream infection originating in the urinary tract. *J Fungi*. 2022;8(2):123. doi:10.3390/jof8020123
39. Kang JH, Super M, Yung CW, et al. An extracorporeal blood-cleansing device for sepsis therapy. *Nat Med*. 2014;20(10):1211–1216. doi:10.1038/nm.3640
40. Herrmann IK, Urner M, Graf S, et al. Endotoxin removal by magnetic separation-based blood purification. *Adv Healthc Mater*. 2013;2(6):829–835. doi:10.1002/adhm.201200358
41. Cohen ND, Cywes-Bentley C, Kahn SM, et al. Vaccination of yearling horses against poly-N-acetyl glucosamine fails to protect against infection with Streptococcus equi subspecies equi. *PLoS One*. 2020;15(10):e0240479. doi:10.1371/journal.pone.0240479
42. Cywes-Bentley C, Rocha JN, Bordin AI, et al. Antibody to Poly-N-acetyl glucosamine provides protection against intracellular pathogens: mechanism of action and validation in horse foals challenged with Rhodococcus equi. *PLoS Pathog*. 2018;14(7):e1007160. doi:10.1371/journal.ppat.1007160
43. Galanzha EI, Shashkov E, Sarimollaoglu M, et al. In vivo magnetic enrichment, photoacoustic diagnosis, and photothermal purging of infected blood using multifunctional gold and magnetic nanoparticles. *PLoS One*. 2012;7(9):e45557. doi:10.1371/journal.pone.0045557
44. Karawacka W, Janko C, Unterweger H, et al. SPIONs functionalized with small peptides for binding of lipopolysaccharide, a pathophysiologically relevant microbial product. *Colloids Surf B Biointerfaces*. 2019;174:95–102. doi:10.1016/j.colsurfb.2018.11.002
45. Ferreira GF, Dos Santos Pinto BL, Souza EB, et al. Biophysical effects of a polymeric biosurfactant in Candida krusei and Candida albicans cells. *Mycopathologia*. 2016;181(11):799–806. doi:10.1007/s11046-016-0054-z
46. Cassone A. Cell wall of Candida albicans: its functions and its impact on the host. *Curr Top Med Mycol*. 1989;3:248–314. doi:10.1007/978-1-4612-3624-5_10
47. Sheppard DC, Locas M-C, Restieri C, Laverdiere M. Utility of the germ tube test for direct identification of Candida albicans from positive blood culture bottles. *J Clin Microbiol*. 2008;46(10):3508–3509. doi:10.1128/JCM.01113-08